

On Signal Attenuation in 5G Higher Frequencies Transmissions with Different Area Scenario

T. Iliev*, I. Stoyanov**, I. Penkov*, G. Mihaylov***, A. Fazylova****, G. Balbayev*****, I. Beloev***** and S. Kosunalp*****

* University of Ruse, Department of Telecommunication, Ruse, Bulgaria

** University of Ruse, Department of Electrical and Power Engineering, Ruse, Bulgaria

*** University of Telecommunications and Post, Department of Telecommunications, Sofia, Bulgaria

**** Almaty University of Power Engineering and Telecommunications named after Gumarbek Daukeyev, Almaty, Kazakhstan

***** Academy of logistics and transport, Almaty, Kazakhstan

***** University of Ruse, Department of Transport, Ruse, Bulgaria

***** Bandırma Onyedi Eylül University, Department of Computer Technologies, Bandırma, Türkiye
tiliev@uni-ruse.bg

Abstract - Energy and cost efficiency are becoming criteria of increasing importance in the design of 5G radio relay lines, especially for areas close to water surfaces, where there is pronounced fading, which is characteristic of radio relay paths that pass on the surface of the water. In this paper, the research was carried out on two radio relay links with different frequencies – the first one at 8 GHz, and the second at 18 GHz, working in frequency diversity mode. To troubleshoot, the measurements were made during the shortest possible time, with fixed emissions to account any fluctuations in signal levels.

Keywords - network planning; 5G; radio – relay line; fading

I. INTRODUCTION

Communication and data transmission systems need a constant increase in bandwidth and data transfer rates. This need is most pronounced in mobile networks. Since 2017, the volume of data traffic in mobile networks has increased several times and is expected to increase in the future as well [1].

Contemporary mobile networks, such as LTE (4G) and 5G, provide users with ever-higher data transfer rates, which inevitably requires ever-increasing bandwidth from transport networks [2]. The fundamental limitations of data rate are due to the bandwidth of the communication system. International organizations, such as CEPT / ECC and ITU-R, dealing with the allocation of the frequency range, allocate a wide frequency range from 6 GHz to 86 GHz for operation of radio relay lines. As the frequency increases, the cost of equipment increases significantly, and the attenuation of signals on surface paths also increases [3]. Therefore, most radio relay communication lines operate in the frequency range up to 30 GHz.

The standard frequency bands for trunk lines are 3.5, 7, 14, 28 and 56 MHz [4].

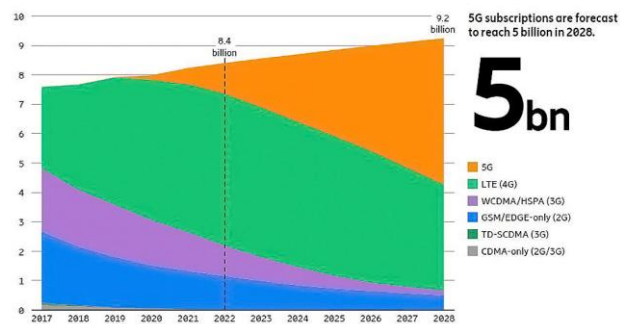


Figure 1. Mobile subscriptions (in billion) [1]

Due to the limited frequency resource, a more efficient use of the allocated frequency band is required; furthermore, the telecommunication operator must be able to increase the bandwidth of the communication line without changing the frequency planning [5].

This paper deals with various ways to improve the efficiency of the use of the frequency resource, as well as the speed of data transmission.

II. RADIO WAVE PROPAGATION

Radio communication is distinguished by the complexity and non-stationarity of the conditions for the propagation of radio waves in inhomogeneous dispersion anisotropic media and interference situations.

Signal fading is characteristic of the HF radio channel. In the ionospheric channel, the signal components propagate along several paths. First, rays are detected at the point of reception, which are propagated by multiple or single reflection. Second, the signal is emitted from the transmitting antenna within the width of the radiation pattern (RP), therefore we can assume that not a single beam falls on the ionosphere, but a beam of sub-beams that reach the receiving antenna with different amplitudes and phases. Third, a propagation medium with large-scale and small-scale inhomogeneous structures leads to

multipath interference. Multipath at high speeds and common types of tampering limit the ability to improve communication reliability by increasing transmitter power [6]. If the difference in the path of the rays is comparable to the duration of one element, then the information is received along the ray that currently has the highest level, and when moving from one ray to another, desynchronization of cycles occurs, which leads to loss of individual symbols of the message. Multipath with a large difference in the path of the beams leads to interference of the message elements arriving at the receiving point with different beams, and the signals in beams with a lower level in this case play the role of additive interference.

Free space is usually considered as a homogeneous, boundless and non-absorbing medium in which the relative dielectric permittivity is equal to one. Thus, many factors affecting the propagation of radio waves are not taken into account. In the Earth's atmosphere, there are always atmospheric gases, water vapor, hydrometeors (cloud, rain, snow, hail, fog), as well as dust particles raised from the Earth's surface, which cause a weakening of the power of the received signal. It is accepted to consider two types of attenuation - absorption and scattering [7]. When absorbed, part of the energy of radio waves is converted into heat energy, and when scattered, it is redistributed in space in directions other than the given one. Attenuation in the troposphere of centimeter range signals is of appreciable value.

$$\bar{P} = \bar{P}_0 10^{-2 \int_0^R \alpha(R) dR}, \quad (1)$$

where R is the distance between transmitter and receiver; \bar{P} is the average power at the receiver input without accounting for attenuation; \bar{P}_0 is the average power at the receiver input, taking attenuation into account; $\alpha(R)$ characterizes the change of the attenuating properties of the medium in the direction of propagation of the radio beam (wave) [8].

In the case of a homogeneous propagation medium, when the attenuation coefficient does not change along the propagation path of the radio waves, the power of the received signal is expressed as:

$$\bar{P} = \bar{P}_0 10^{-2\alpha R}, \quad (2)$$

where α is attenuation coefficient (dB/km).

When using a logarithmic scale, (2) will convert to:

$$10 \lg \frac{\bar{P}}{\bar{P}_0} = -2\alpha R. \quad (3)$$

To characterize the total loss along the propagation path, the coefficient Γ is introduced. The value of α is measured in decibels (dB) and is the sum of the attenuation coefficients in gasses and water vapor α_g , in clouds α_c and precipitation α_p :

$$\Gamma = 2(\alpha_g \Delta r_g + \alpha_c \Delta r_c + \alpha_p \Delta r_p), \quad (4)$$

A. Free Space Communications

The transmission in free space can be represented by the Friis formula (5):

$$\frac{P_r}{P_t} \approx \left(\frac{\lambda}{4\pi d} \right)^2 \quad (5)$$

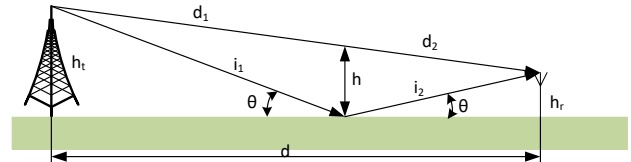


Figure 2. Direct and reflected signal on flat terrain

The attenuation of the signal when reflected from the earth's surface can be represented by:

$$\frac{P_r}{P_t} \approx \left(\frac{h_t h_r}{d^2} \right)^2, \quad (6)$$

where P_r is received power; P_t is radiated power; d is the distance between receiver and transmitter; h_t , h_r are the heights of transmitting and receiving antenna respectively.

When propagating in free space, attenuation of the signal may be present at sharp edges (knife - edge diffraction loss) - a wedge-shaped obstacle. These obstacles can be due to hills, buildings, trees, etc. obscuring the radio path and line-of-sight (LoS) beam. In this way, a "shadowing" effect appears on the receiver [9].

There are several different variations of signal attenuation from multiple wedge-shaped obstacles:

- Bullington model - attenuation by 2 obstacles. N obstacles are replaced by one of equivalent height h , reflecting the effect of all wedge-shaped obstacles (some obstacles are ignored) [6].

The diffraction parameter v is defined as:

$$v = h \sqrt{\frac{2}{\lambda} \left(\frac{1}{d_1} + \frac{1}{d_2} \right)}, \quad (7)$$

where h is the height of the obstacle, d_1 is distance transmitter - obstacle; d_2 is distance receiver - obstacle

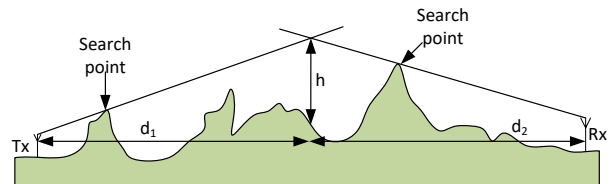


Figure 3. Bullington model

- Epstein-Peterson model – it considers the attenuation from each obstacle sequentially, with the total attenuation being the sum of the individual attenuations [6].

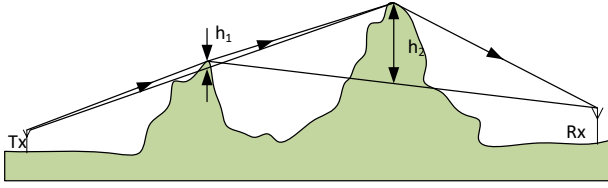


Figure 4. Epstein-Peterson model

- Deygout model – the model initially considers the damping effect of the main obstacle, and the effect of other obstacles relative to it [6].

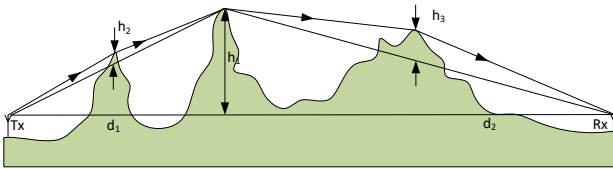


Figure 5. Deygout model

B. Attenuation of centimeter radio waves in atmosphere and vapor

Attenuation is due to the scattering and absorption of signal energy due to the conversion of some of the energy into thermal energy by gas particles (oxygen and nitrogen) and water vapor.

In the propagation of radio waves with a wavelength smaller than $\lambda = 3.2$ cm, the attenuation in the troposphere is mainly due to absorption, the scattering effect is insignificant and can be neglected [9]. Then the total attenuation coefficient α_T is the sum of the attenuation coefficients of the gas and water vapor:

$$\alpha_T = \alpha_g + \alpha_w, \quad (8)$$

where α_g and α_w are the attenuation coefficients (dB/km) of gas and water vapor, respectively.

C. Attenuation of centimeter radio waves in presence of rain

Rain consists of water particles of various sizes, shapes and densities. Due to the fact that the size distribution law is different for different particle sizes, the most appropriate method for calculating the attenuation coefficient is the empirical method, where it is assumed that the dependence of the attenuation coefficient on the intensity of precipitation is an exponential law:

$$\alpha_c = aI^b, [dB/km], \quad (9)$$

where the parameters a and b are empirical values and which depend on the wavelength (e.g., at $\lambda=3.2$ cm $a=0.0074$ and $b=1.31$); I - precipitation intensity [mm/h].

D. Attenuation of centimeter radio waves in presence of snowfall

The snowflakes that make up snowfall vary in shape, orientation, density, size, and moisture content. Most snowflakes are hexagonal and range from 0.5 to 3 mm in diameter. The refractive index is the combined index for a mixture of air, water and ice [10]. If we assume that the snowflake has a spherical shape and its mass is equal to the mass of the same water sphere, it is possible to calculate the damping coefficient of liquid snow by the snowfall intensity I by means of:

$$\alpha_c = 0.094 \frac{I}{\lambda}. \quad (10)$$

For dry snowfall at 0°C, the attenuation coefficient is described by:

$$\alpha_n = 0.035 \frac{I^2}{\lambda^4} + 0.0022 \frac{I}{\lambda}. \quad (11)$$

In conclusion, it can be said that the magnitude of the attenuation coefficient in the millimeter range is much larger than in the centimeter range; when operating at short distances, attenuation in gases and clouds without precipitation can be neglected; it is necessary to take into account only the attenuation of the signal in heavy rain, hail and snowfall [11].

III. STUDY OBJECTS

Three routes differing in type of terrain and altitude were investigated.

A. Trace route 1: Dospat - Sarnitsa.

The length of the track is 15.6 km. The landscape is mountainous, highly dissected and rounded. The average altitude is 1,300 m. For the lower parts of the territory, the annual amount of precipitation is from 620 to 700 l/m², and for the higher ones from 780 to 1100 l/m². The average snow cover is about 97 cm and lasts between 80 and 150 days. The average atmospheric pressure for the Smolyan region is 737.0 hPa. The average annual temperature ranges from 9 to 13°C. The forms of the relief in this part have a significant impact on the radio relay connection and the relatively high altitude (1000 - 1600 m) in the territory creates conditions for almost daily temperature inversions and the air temperatures throughout the year are much lower than places with a similar height in the rest of the mountains.



Figure 6. Dospat – Sarnitsa [12]



Figure 7. Dyuni – St. Toma [13]

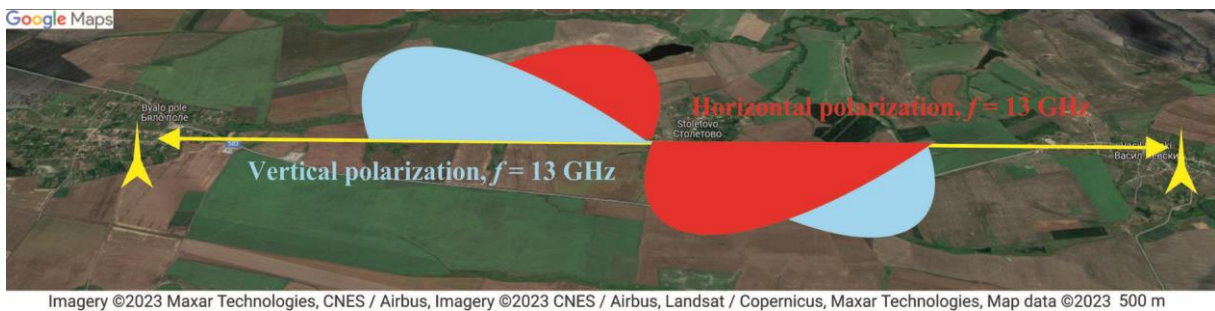


Figure 8. Opan – Vasil Levski [14]

B. Trace route 2: Dyuni – St. Toma

The second route is located on the coast of the Black Sea with geographical coordinates 42.3704473, 27.705076. The track is deployed entirely above sea level. The coast is highly fragmented, with a large part occupied by sand dunes. The region's climate is midway between humid subtropical and Mediterranean, with relatively warm but windy winters (average January temperature +6 °C) and long, warm summers (average July temperature +27 °C). The Black Sea is the main formative factor. The adjacent sea basin causes year-round high air humidity.

C. Trace route 3: Opan – Vasil Levski

The geographical position of the track is 42°10' north latitude and 25°23' east longitude, which shows almost

equal proximity to the Equator and to the North Pole, which in terms of climate implies moderate values. The average altitude is 157.8 m, with the highest point being 192 m in the land of the village of Vasil Levski. The landscape is characterized as flat and slightly hilly. The route area falls within the transitional-continental climate sub-region of the European-continental climate region. The climate is warm, moderately humid. The area is characterized by good radiation characteristics. The average annual air temperature in the area is +11.4 °C, and all winter average monthly temperatures are positive. The average January temperature is + 1 °C.

In the atmosphere, especially during the winter months, there are significant sources of emissions that pollute the air - an increased concentration of soot in the air.

IV. MAIN RESULTS AND ANALYSIS

In order to troubleshoot the three tracks in question, measurements were taken at short time intervals. The levels of the broadcast signals are fixed on both sides of the track, the aim being to register more clearly the fluctuations in the signal levels. The automatic transmit power control (ATPC) in our investigations is stopped.

Dospat - Sarnitsa is a radio relay route that is of utmost importance for the construction of a reliable and secure mobile network that provides mobile services to small but important regions.

The following solutions were initially used for the construction of the route: dipole antennas, at a frequency of 7GHz with a size of 0.6 meters. Operating in vertical polarization mode. Adaptive modulation, with the minimum modulation being 45Mbit/s- 16QAM and the maximum being 80 Mbit/s- 256QAM. The channel spacing is 14MHz. The broadcasting frequency from Dospat in the direction of Sarnitsa is 7.779750 GHz and the broadcasting frequency from Sarnitsa in the direction of Dospat is 7.928250 GHz. Transmission (Tx) is 20dBm and receive levels of -47dBm are expected under normal conditions. The maximum transmit power is 26dBm and -55dBm far end input power is set for the route target (Fig. 9).

After upgrading the generations of the mobile network from 4G to 5G, a parallel link was deployed at 18 GHz, which works in Frequency Diversity mode. Ultra high performance dual polarized 0.6 meter antennas are used. The size of the antennas is adapted to the length of the route. Adaptive modulation is used, with the minimum modulation being 4QAM - 21Mbit/s and the maximum being 64QAM - 64 Mbit/s. The channel spacing is 14MHz; The broadcast frequency in one direction from Dospat to Sarnitsa is 17.906250 GHz, and the broadcast frequency in the opposite direction from Sarnitsa to Dospat is 18.916250 GHz.

The measured reception levels of RRL Dospat - Sarnitsa are presented in Fig. 9. The radio relay route passes over the Dospat Dam (Fig. 6) and has pronounced fadings, which are characteristic of radio relay routes that pass on the water surface (Fig. 9). Transmit (Tx) is 19dBm and under normal conditions expected receive levels are around -49dBm.

There are two links deployed above the dam. One link operates at 8 GHz, and the other at 18 GHz, in frequency diversity mode, and in practice a separate link is established to carry the same traffic in the presence of fading.

Trace routes Sarnitsa – Dospat and Dyuni – St. Toma are deployed using frequency diversity, and radiolink (RL) Vasil Levski (Tx) – Opan is deployed using XPIC technology.

On trace route 3 Opan - Vasil Levski, data traffic is transmitted at 13 GHz using XPIC technology (Fig. 11). The observed fadings are at the same time for both horizontal and vertical polarization of the signal.

In the diagrams (Fig. 9, Fig. 10 and Fig. 11) distinct fadings are observed. Fadings are observed in the morning

when there is an inhomogeneous environment, moisture, vapors, etc. at which the radio waves decay. Most often, this phenomenon is observed in the time range from 3 AM to 7 AM. This signal dropout depends on the carrier frequency.

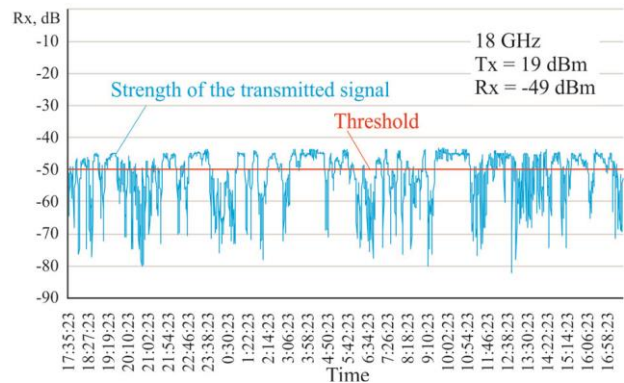
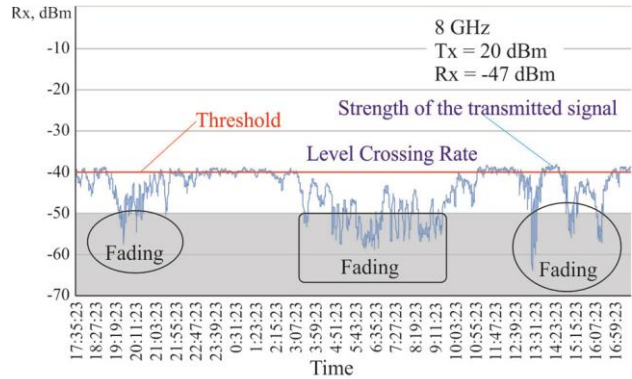


Figure 9. Fading casses of radiolink (RL) Sarnitsa (Tx) – Dospat (Rx)

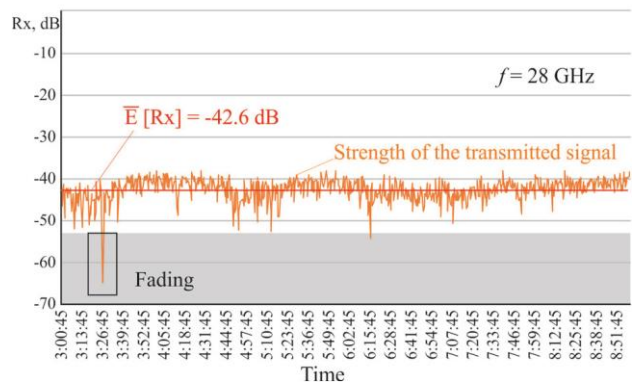
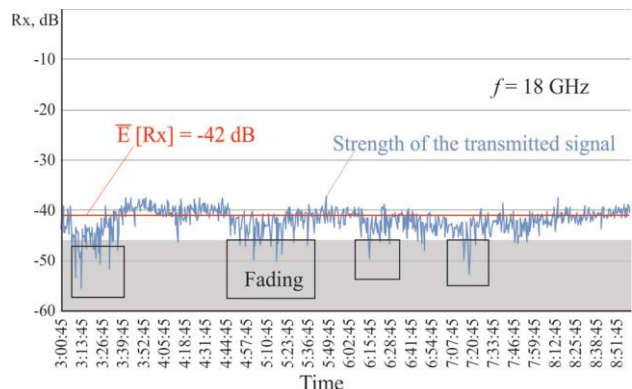


Figure 10. Fading casses of frequency diversity RL Dyuni (Tx) – St. Toma (Rx)

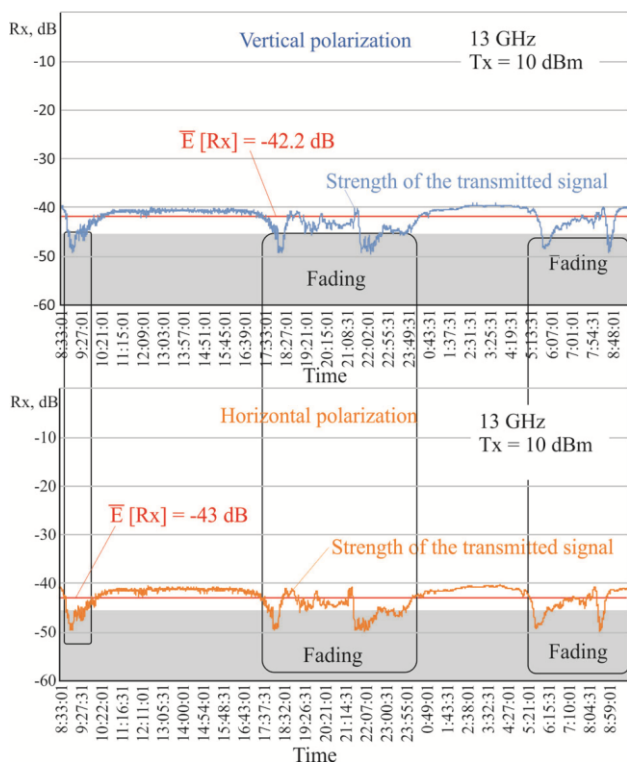


Figure 11. Fading cases of XPIC RL Vasil Levski (Tx) – Opan (Rx)

The difference in the signal drops for the trace routes above water surface (trace route 1 and trace route 2) using frequency diversity is greater compared to the fading for trace route 3 (built on flat terrain). For the 8 GHz traces, the frequency of observed fading is higher than the traces operating at a higher frequency (18 and 28 GHz).

V. CONCLUSION

Three different radio relay routes for a 5G network, differing in type of terrain and altitude, are considered in the work. By troubleshooting the three RRL routes in question and measuring the signal level in the shortest possible time. Low signal reception levels lead to loss or reduction of path capacity. 5G generation networks aim for 99.99% track availability. For that reason, frequency diversity technology has been applied, which uses the more stable frequency for transmission, which can be different from the one for reception. In such a system, attenuations are a rare event. If each link has a drop/loss probability of 1% or 0.01, the probability of both links dropping at the same time would be $0.01 \times 0.01 = 0.0001$ or 0.01%.

It would be good to have one of the tracks at a higher frequency, as higher frequencies such as 24, 26, 28, 30, 32 GHz are more resistant to fading. On the other hand, radio frequency spectrum is regulated by national and international regulations to ensure that social and economic benefits are maximized, therefore it is limited.

ACKNOWLEDGMENT

This work is also partially supported by the EC Project 2020-1-PL01-KA226-HE-096196, project title: “Holistic

approach towards problem-based ICT education based on international cooperation in pandemic conditions”.

REFERENCES

- [1] Ericsson Mobility Report, November 2022, available at: <https://www.ericsson.com/en/reports-and-papers/mobility-report/reports/november-2022> [Access on 15 February 2023]
- [2] S. Kostadinova, V. Markova, N. Kostov, I. Balabanova and G. Georgiev, "Latency Analysis for 5G Optical Transport Network," 2021 International Conference on Biomedical Innovations and Applications (BIA), Varna, Bulgaria, 2022, pp. 9-12, doi: 10.1109/BIA52594.2022.9831249.
- [3] S. Sadinov, P. Kogias, K. Angelov, M. Malamatoudis and A. Aleksandrov, "The Impact of Channel Correlation on the System Performance and Quality of Service in 5G Networks," 2020 7th International Conference on Energy Efficiency and Agricultural Engineering (EE&AE), Ruse, Bulgaria, 2020, pp. 1-4, doi: 10.1109/EEAE49144.2020.9278982.
- [4] ETSI EN 302 217-1 V2.0.0, Fixed Radio Systems; Characteristics and requirements for point-to-point equipment and antennas; Part 1: Overview and system-independent common characteristics, 2012-09, available at: https://www.etsi.org/deliver/etsi_en/302200_302299/30221701/02.00.00_20/en_30221701v020000c.pdf [Accessed 10 February 2023]
- [5] H.-Yi Chen and D.-P. Lin, "Volume integral equation solution of microwave absorption and scattering by raindrops," IEEE Antennas and Propagation Society International Symposium, Orlando, FL, USA, 1999, pp. 2676-2679 vol.4
- [6] M. J. Conway, C. J. Payne, S. G. Bilén and E. N. Koski, "Ground-wave propagation characterization and prediction for HF cognitive radio," 2015 IEEE Military Communications Conference, Tampa, FL, USA, 2015, pp. 1643-1649
- [7] T. Iliev, T. Bikov, G. Mihaylov, E. Ivanova, I. Stoyanov, V. Keseev, Algorithms for Congestion Control in LTE Mobile Networks. In: Silhavy, R. (eds) Software Engineering and Algorithms in Intelligent Systems. CSOC2018 2018. Advances in Intelligent Systems and Computing, vol 763. Springer, Cham. https://doi.org/10.1007/978-3-319-91186-1_49.
- [8] A. Haka, R. Vasilev, V. Aleksieva and H. Valchanov, "Simulation Framework for Building of 6LoWPAN Network," 16th Conference on Electrical Machines, Drives and Power Systems (ELMA), Varna, Bulgaria, 2019, pp. 1-5, doi: 10.1109/ELMA.2019.8771633.
- [9] G. Mihaylov and E. Ivanova, "Analysis and Estimation of the Field Strength of Digital Terrestrial Television Broadcasting", The Journal of CIEES, vol. 1, no. 1, pp. 17–22, Jun. 2021. DOI:<https://doi.org/10.48149/jciees.2021.1.1.3>.
- [10] H Valchanov, J Edikyan, V Aleksieva , A Study of Wi-Fi Security in City Environment, IOP Conf. Ser.: Mater. Sci. Eng. 618 012031, DOI: 10.1088/1757-899X/618/1/012031
- [11] K. Angelov and S. Sadinov, "Modelling and Simulation Analysis of Routing Algorithms in Multichannel Optical Communication Networks", The Journal of CIEES, vol. 1, no. 1, pp. 29–33, Jun. 2021. DOI:<https://doi.org/10.48149/jciees.2021.1.1.5>.
- [12] Google Maps. "Dopat" Satellite image. 2023, <https://www.google.bg/maps/place/4831+%D0%94%D0%BE%D1%81%D0%BF%D0%B0%D1%82/@41.6916978,24.0538651,10703m/data=!3m1!1e3!4m5!3m4!1s0x14ac785d454f4b53:0x85a9948f2f675ac4!8m2!3d41.645973!4d24.1595237?hl=bg&authuser=0>. [Accessed 17.02.2023]
- [13] Google Maps. "Dyuni" Satellite image. 2023, <https://www.google.bg/maps/place/8130+%D0%94%D1%8E%D0%BD%D0%B8/@42.3587088,27.6966507,6672m/data=!3m1!1e3!4m5!3m4!1s0x40a6c892563a9ed3:0x40f61ec479a734d2!8m2!3d42.3704473!4d27.705076?hl=bg&authuser=0>. [Accessed 17.02.2023]
- [14] Google Maps. "Opan" Satellite image. 2023, <https://www.google.bg/maps/place/6078+%D0%9E%D0%BF%D0%B0%D0%BD/@42.1699582,25.6643101,15024m/data=!3m1!1e3!4m5!3m4!1s0x40a808978eb7a279:0x400a01269bf5af0!8m2!3d42.2108979!4d25.6882893?hl=bg&authuser=0>. [Accessed 17.02.2023]